Available online at http://www.journalcra.com

International Journal of Current Research
Vol. 5, Issue, 07, pp.1670-1676, July, 2013

INTERNATIONAL JOURNAL OF CURRENT RESEARCH

ISSN: 0975-833X

RESEARCH ARTICLE

INVESTIGATION OF HEXAVALENT CHROMIUM [Cr(VI)] REMOVAL BY CARBOXYMETHYL CELLULOSE STABILIZED ZEROVALENT IRON NANOPARTICLES

Selvarani Murugan and Prema Paulpandian*

Department of Zoology, VHNSN College (Autonomous), Virudhunagar – 626 001. Tamil Nadu, India

ARTICLE INFO

Article History:
Received 14th April, 2013
Received in revised form
21st May, 2013
Accepted 18th June, 2013
Published online 18th July, 2013

Key words:

Adsorption isotherms,
Diphenylcarbazide,
Reaction kinetics,
Removal efficiency,
Spectrophotometer.

ABSTRACT

The use of zero-valent iron nanoparticles (nZVI) has been gained increasing interest in the area of environmental remediation. Hence the present attempt has been aimed to investigate the removal efficiency of Cr(VI) by adsorption on carboxymethyl cellulose stabilized zero-valent iron nanoparticles (CMC-Fe^o) from aqueous solutions under different experimental conditions. Nanoparticles were synthesized by reducing Ferrous sulfate heptahydrate ($FeSO_4.7H_2O$) using sodium borohydride ($NaBH_4$) in the presence of CMC as a stabilizer. The crystalline size of the respective particles was determined through X-ray diffractogram (XRD) and the size of the particle was found to be 10.77 nm. Morphology of the particles was observed using scanning electron microscopy (SEM). Fourier transform infrared (FTIR) spectroscopy results suggested that stabilizer molecules were adsorbed to iron nanoparticles resulting in a steric layer, and thereby, preventing the nanoparticles from agglomeration. The removal efficiency of Cr(VI) was found to be increased with decrease of Cr(VI) concentration (10 mg/L – 25 mg/L) and pH (3 – 10) and inversely with increase in Fe^o concentration (0.1 g/L – 0.4 g/L) and temperature (15^oC – 45^oC). The obtained data revealed that the adsorption of Cr(VI) onto CMC stabilized Fe^o nanoparticles which were found to fit well by the Freundlich isotherm. The kinetic models were then examined with pseudo first order rate reaction. The correlation coefficient between experimental parameters and time showed that there is a strong positive correlation for Cr(VI) reduction. These results suggest that CMC stabilized Fe^o nanoparticles could be employed as an effective adsorbent for the removal of chromium (Cr) from contaminated water

INTRODUCTION

The increasing contamination of urban and industrial waste waters by toxic metal ions is a worrying environmental problem. Chromium (Cr) is one of the concerned heavy metals due to its high toxic and carcinogenic properties. It is commonly found in waste water from electroplating and metal finishing processes, pigment manufacturing, tannery facilities and chrome mining operations. In the United States, it is the second most common inorganic contaminant in water after lead (Wielinga *et al.,* 2001). In aqueous environment, Cr usually exists in hexavalent [Cr(VI)] and trivalent [Cr(III)] forms. Cr(III) is much less soluble and relatively stable. However, Cr(VI), such as chromate (CrO_4^{2-}, $HCrO_4$) and dichromate ($Cr_2O_7^{2-}$) are highly soluble and mobile in aqueous solutions. The hexavalent form has been considered more hazardous to public health due to its mutagenic and carcinogenic properties (Basha *et al.,* 2008). Due to the toxicity and carcinogenicity of Cr(VI), the U.S. Environmental Protection Agency (EPA) has set the maximum level of total chromium concentration allowed in drinking water at 0.1 mg/L (Lazarids and Asouhidou, 2003). Therefore, reduction of Cr(VI) to Cr(III) has been considered as an important remediation technology for Cr(VI) contaminated soil and water. Shen *et al.* (2012) investigated that Cr(VI) removal capacity highly depended on reaction time, solution pH, temperature, initial Cr(VI) concentration and material dosage.Various methods of chromium removal include filtration, chemical precipitation, adsorption, electrodeposition and membrane system or even ion exchange process. Among them, adsorption is one of the most economically favorable and a technically easy method (Karthikeyan *et al.,* 2005). Over the last several years, a variety of adsorbents have been used for chromium removal from contaminated soil and water. Nano iron particles are particularly attractive for remediation purposes due to their significant surface area to volume ratio leading to a greater density of reactive sites and heavy metal removal capacity. In the conventional borohydride reduction method (Wang and Zhang, 1997), ZVI nanoparticles are prepared by reducing ferrous or ferric ions with borohydride in water. A number of physico chemical processes can affect the formation and size of the resultant ZVI clusters, including inter-particle interactions and particle nucleation and thus, nanoparticle agglomerates rapidly. When a stabilizer is applied, the stabilizer molecules are absorbed to the surface of the particles, preventing further agglomeration. In addition, the presence of a stabilizer may facilitate the nucleation and growth of iron particles during the formation of nanoparticles (Shimmin *et al.,* 2004). To implement the *in-situ* injection of Fe nanoparticles, an ideal stabilizer should be a) able to specifically interact with the nanoparticles and hence suppress their growth; b) environmentally benign; c) cost-effective; and d) mobile in soils.

Recently, He and Zhao (2005) reported that a food-grade water-soluble starch can improve both dispersibility and reactivity of Fe nanoparticles. Unfortunately, the starched Fe particles became less stable as evidenced by the appearance of floc precipitates after 2 days, thereby limiting long-term storage and commercial application of these Fe nanoparticles. Therefore, a better stabilizer with stronger interaction with Fe particles needs to be developed that will allow longer-lasting effective stabilization and facilitate environmental applications of these nanoparticles. To prepare physically more stable and chemically more reactive Fe^o based nanoparticles, poly acrylic acid (PAA) employed as supports for iron and bimetallic nanoparticles (Ponder *et al.,* 2001; Schrick *et al.,* 2002; Zhu *et al.,*

Corresponding author: Prema Paulpandian
Department of Zoology, VHNSN College (Autonomous), Virudhunagar – 626 001. Tamil Nadu, India

2006). These supports prevented iron nanoparticles from agglomeration and thereby prolonged the reactivity of the particles. Generally, polymers such as CMC, guar gum, chitosan, and PAA provide steric stabilization that exhibit a larger repulsion force than electrostatic repulsion (Geng *et al.,* 2009), hence they can help to stabilize Fe^o nanoparticles (Tiraferri and Sethi, 2008) and superparamagnetic ferrofluid (Lin *et al.,* 2005) via carboxylate binding. CMC is a water soluble, food-grade ingredient, nontoxic and biodegradable, low cost and environmentally friendly likely due to the presence of highly biodegradable –OH, -CO-, and –COOH groups. CMC has been successfully used as an effective stabilizer in preparing nanoparticles such as superparamagnetic iron oxide nanoparticles and Ag nanoparticles (Magdassi *et al.,* 2003; Si *et al.,* 2004). CMC is a polyelectrolyte and carries carboxylate groups in addition to hydroxyl groups. Consequently, CMC is expected to interact with Fe nanoparticles more strongly and stabilize the nanoparticles more effectively. The primary objective of this work is to prepare a new class of Fe^o nanoparticles involving the use of an innocuous stabilizer and to test the ability of such particles to remove Cr(VI) from aqueous solution. Influence of Cr(VI) concentration, nanoparticles concentration, variation in pH, temperature and different types of Fe^o nanoparticles on the removal efficacy of Cr(VI) were also evaluated. The obtained experimental data was then fitted with Langmuir and Freundlich adsorption isotherm models and rate constant kinetic reactions.

MATERIALS AND METHODS

Materials

Ferrous sulfate heptahydrate ($FeSO_4.7H_2O$), Sodium borohydride ($NaBH_4$), Sodium Carboxy Methyl Cellulose (NaCMC) and Ethanol were purchased from Himedia (P) Ltd, Mumbai were used as starting materials without further purification. Potassium dichromate ($K_2Cr_2O_7$) was used as a model contaminant. Milli-Q water was used throughout the experiment.

Methods

Preparation of CMC-Fe^o nanoparticles

The preparation of CMC-Fe^o nanoparticles was followed the method reported by He and Zhao (2005). In brief, the preparation was carried out in a 250 ml flask attached to a vacuum line. Before use, deionized (DI) water was purged with purified nitrogen (N_2) gas for 15 min to remove dissolved oxygen (DO). In a typical preparation, a stock solution of 0.21 M $FeSO_4.7H_2O$ was prepared right before use. Fe concentration used in this study was 0.1 g/L and the corresponding CMC concentration was 0.2% (w/v). The Fe^{2+} ions were then reduced to Fe^o by adding a stoichiometric amount of $NaBH_4$ aqueous solution at a BH_4^-/Fe^{2+} molar ratio of 2.0 to the mixture with magnetic stirring at 230 rpm under ambient temperature. The ferrous ion was reduced to zero-valent iron according to the following reaction:

$$Fe(H_2O)_6^{2+}+2BH_4^-\rightarrow Fe^0\downarrow+2B(OH)_3+7H_2\uparrow$$

The resultant black particles were separated from the solution by centrifugation at 4000 rpm for 5 min and washed with N_2 saturated deionized water and at least three times with 99% absolute ethanol. Finally, the synthesized Fe^o nanoparticles were dried in an oven at 60°C. The dried particles were used for further analysis.

Characterization of synthesized CMC-Fe^o nanoparticles

FTIR spectroscopy

To analyze the modes of interaction between CMC and the nanoparticle surface, FTIR spectroscopy measurements were carried out. The FTIR spectra of the CMC and nanoparticles were recorded in the transmission mode at room temperature using potassium bromide (KBr) pellet technique (1:20). The KBr was dried in a dryer at 200°C for 24 h, then 560 mg KBr was homogenized with sample and ground afterward to fine powder with a mortar and pestle. Shimadzu (Japan) infrared spectrophotometer was used to determine the spectra of the sample in the spectral range between 500 and 4,000 cm^{-1}.

X-ray diffractogram

XRD patterns of synthesized nanoparticles were recorded with an X'pert PROPAN analytical instrument operated at 40 kV and a current of 30 mA with Cu α radiation (λ=1.54060 Å). A continuous scan mode was used to collect 2θ data from 10.08° to 79.93°. The diffraction intensities were compared with the standard JCPDS files. Crystalline size of the nanoparticles was calculated from the line broadening of X-ray diffraction peak according to the Debye-Scherer formula

$$D = k\lambda/ \beta \cos\theta,$$

Where D is the thickness of the nanocrystal, 'k' constant, 'λ' wavelength of X-rays, 'β' width at half maxima of reflection at Bragg's angle 2θ, 'θ' Bragg's angle.

Scanning electron microscopy

Size and morphology of the nanoparticles was examined by SEM (SU 1510) operated at 5 kV, magnification x10 k. Thin film of the sample was prepared on a carbon coated copper grid by just dropping the suspension of nanoparticles in water on the grid, extra solution was removed using blotting paper and then the film on the SEM grid were allowed to dry by putting it under a mercury lamp for 5 min. The sample surface images were taken at different magnifications.

Cr(VI) reduction studies

Preparation of Cr(VI) solution

Stock solution (1000 mg/L) of Cr(VI) was prepared by dissolving 2.829 g of $K_2Cr_2O_7$ in 1000 ml of deionized water. Experimental solutions of the desired concentrations were obtained by successive dilutions with deionized water, and pH was adjusted to the desired values according to the following experimental design with 0.1 M NaOH or HCl solutions.

Adsorption experiments

Adsorption experiments were conducted to evaluate the removal rate of Cr(VI) in the presence of CMC stabilized Fe^o nanoparticles as adsorbent. The experiments for the reduction of Cr(VI) was performed in 250 ml Erlenmeyer flasks into which synthesized CMC stabilized Fe^o nanoparticles were introduced, followed by the addition of $Cr_2O_7^{2-}$ aqueous solution. The reaction mixture was kept at a stirring speed of about 500 rpm. The samples were withdrawn periodically by glass syringe and filtered immediately through nitrocellulose membrane filter paper (0.2 μm). The filtrates were analyzed for residual Cr(VI) concentration by reaction with 1,5-diphenylcarbazide followed by absorbance measurement at 540 nm using UV-Vis spectrophotometer. The influence of various parameters namely Cr(VI) concentration, Fe^o concentration, pH, and temperature on the Cr(VI) reduction was studied. Fe^o nanoparticles concentration used in this study was 0.1 g to 0.4 g/L. The Cr(VI) concentration was 10 mg/L to 25 mg/L, the pH was 3 to 10 and the temperature was 15°C to 45°C.

Removal efficacy of Cr(VI) by CMC-Fe^o nanoparticles

Removal efficacy is defined as the fraction of Cr(VI) in the solution during the reaction time as a fraction of the initial concentration. The percentage removal efficacy of Cr(VI) was calculated spectrophotometrically using the formula,

$$\text{Percentage Removal of Cr(VI)} = \frac{Co-Ce}{Co} X100$$

Where, C_o and C_e represent initial and final concentration of Cr(VI).

Adsorption kinetics

The amount of Cr(VI) adsorbed by CMC stabilized Fe^o nanoparticles was calculated from the difference between Cr(VI) reduction at an initial and equilibrium state, q_e was calculated by

$$q_e = (C_o - C_e) \text{ X } V/M$$

Where q_e (mg/g) is the amount of adsorbed Cr(VI) onto adsorbent, C_o (mg/L) the initial Cr(VI) concentration, C_e (mg/L) the Cr(VI) concentration after a certain period of time t, V (L) the volume of solution and M (g) the mass of the adsorbent used. The kinetic model of Cr(VI) reduction by Fe^o nanoparticles can be described using the pseudo-first order kinetic equation (Franco *et al.,* 2009). The linearized form of pseudo-first order model for the adsorption of Cr(VI) ions onto CMC stabilized Fe^o nanoparticles is given as follows

$$\log(q_e - q_t) = \log q_e - \frac{k1}{2.303} t$$

where q_e and q_t are the amounts of adsorbed Cr(VI) on the adsorbent at equilibrium and at time t respectively (mg/g), and k_1 is the first-order adsorption rate constant (min^{-1}).

Adsorption isotherm models

Adsorption isotherm studies are important to determine the efficacy of adsorption. An adsorption isotherm models describes the fraction of sorbate molecules that are partitioned between liquid and solid phases at equilibrium (Hu *et al.,* 2011). Several adsorption isotherms models are adopted to correlate adsorption equilibrium in heavy metals adsorption. In this study, most commonly used Langmuir and Freundlich isotherm models are used to determine the adsorption equilibrium between the adsorbent and metal ions.

Langmuir isotherm

The Langmuir isotherm model assumes that a monomolecular layer is formed when adsorption takes place without any interaction between the adsorbed molecules (Aksu, 2002). The linearized form of the Langmuir equation is expressed as follows

$$\frac{C_e}{qe} = \frac{1}{q_m K_q} + \frac{1}{q_m} C_e$$

where C_e is the equilibrium concentration (mg/L), q_e the amount of metal ion sorbed (mg/g), q_m is q_e for a complete monolayer (mg/g). K_q is a constant related to the affinity of the binding sites (L/mg).

Freundlich isotherm

The Freundlich isotherm is an empirical equation assuming that the adsorption process takes place on heterogeneous surfaces and adsorption capacity is related to the concentration of Cr(VI) at equilibrium (Li *et al.,* 2005). The linearized form of the Freundlich equation is expressed as follows

$$\log q_e = \log K_f + \frac{1}{n} \log C_e$$

where q_e and C_e are the equilibrium concentration of Cr(VI) in the adsorbed (mg/g) and liquid phases (mg/L) respectively, K_f and n are the Freundlich constants which are related to adsorption capacity and intensity respectively.

RESULTS AND DISCUSSION

Characterization of synthesized CMC-Fe^o nanoparticles

FTIR spectroscopy

The binding interaction of CMC with Fe^o nanoparticles was investigated using FT-IR studies. The FT-IR spectra of CMC alone and CMC stabilized Fe^o nanoparticles are given in Fig.1. The band at 3,327 cm^{-1} was ascribed to OH stretching vibration and the one at 1,642 cm^{-1} to the OH bending vibration of surface-adsorbed water. The stretching bands of the hydroxyl group shifted from 3,328 cm^{-1}

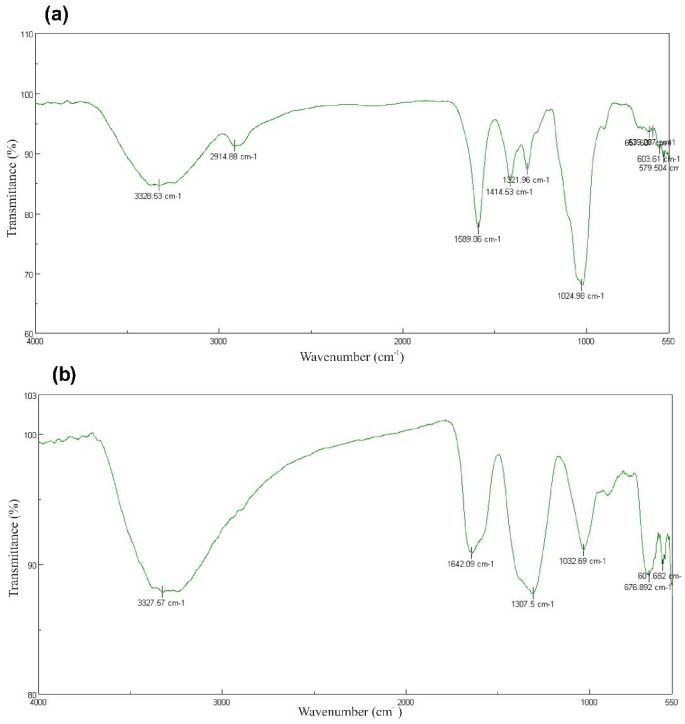

Fig.1. FT-IR spectra of (a) CMC and (b) CMC stabilized Fe^o nanoparticles

for CMC to 3,327 cm^{-1} for CMC-Fe^o and a noticeable decrease in the wave number indicating that the O-H vibration were affected due to the iron attachment. He *et al.* (2007) reported that due to the abundance of –OH groups in CMC, binding of CMC to Fe^o nanoparticles is facilitated only through this group. Similar

observations were noticed by some other researchers (Geng *et al.,* 2009).

X-ray diffraction

The XRD pattern shows that the synthesized CMC stabilized Fe^o nanoparticles are in amorphous stage and in tetragonal system. In the respective nanoparticles, the intensive diffraction peaks were observed at a 2θ value of 44.7° from the lattice plane (110) of face-centered cubic (fcc) Fe unequivocally indicates that the particles are made of pure iron (Fig.2). Singh *et al.* (2011) reported that characteristic peak at 2θ value of 44.751° indicates the crystalline nature of Fe^o nanoparticles and our results corroborate with this findings. In the obtained spectrum, the Bragg's peak position and their intensities were compared with the standard JCPDS files. The size of the particles was found to be 10.74 nm.

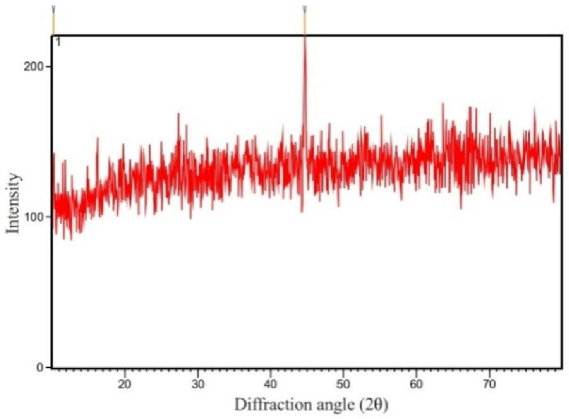

Fig.2. X-ray diffraction spectrum of CMC stabilized Fe^o nanoparticles

Scanning electron microscopy

The scanning electron micrograph of nanoparticles shows that the particles are spherical in nature (Fig.3). The micrograph shows that the synthesized particles did not appear as discrete particles but form much larger dendritic flocs. The aggregation is attributed due to the vandar waals forces and magnetic interactions among the particles. This finding is very much closer to the earliest report (Yuvakumar *et al.,* 2011).

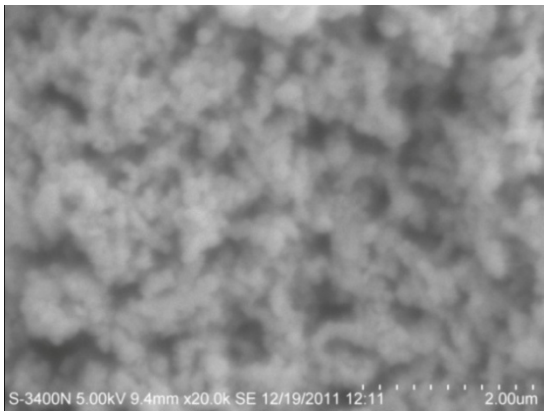

Fig.3. Scanning electron mircograph of CMC stabilized Fe^o nanoparticles

Stability test of CMC-Fe^o nanoparticles

To examine the stability of CMC stabilized Fe^o nanoparticles, batch sedimentation experiments were carried out. For that, nanoparticle suspension of bare and CMC stabilized Fe^o nanoparticles were transferred to quartz cell is shown in Fig.4. The nanoparticles prepared without CMC settled at the bottom of the tubes is less than 20 min while the CMC stabilized Fe^o nanoparticles remained in suspension over a period of more than 1 week with no noticeable precipitation. These results confirmed that the presence of CMC prevented agglomeration of the resulting Fe^o nanoparticles and thus maintained the high surface area and potential reactivity of the particles.

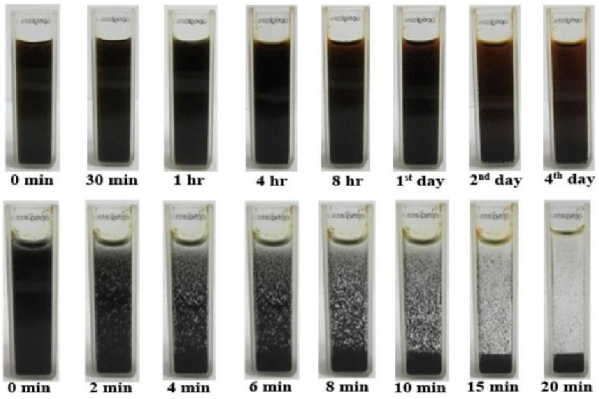

Fig.4. Tubes containing CMC stabilized Fe^o nanoparticles (upper) and Fe^o nanoparticles alone (lower) for the assessment of stability study

Cr(VI) reduction studies

Effect of Cr(VI) concentration

The initial concentration of metal ion provides an important driving force to overcome all mass transfer resistances of metal ions between the aqueous and solid phases (Malkoc, 2006). Fig.5 represents the effect of different initial Cr(VI) concentration (10 mg/L to 25 mg/L). This clearly shows that as metal ion concentration increases, there is a gradual decrease in the percentage removal of Cr(VI). The removal rate was 71.6% at a concentration of 25 mg/L and 94.0% at the lowest initial concentration of 10 mg/L. The removal fraction of Cr(VI) decreased with an increase in the Cr(VI) concentration is due to the fact that nZVI had a limited active sites, which would have become saturated above a certain concentrations (Wang *et al.,* 2009). Calculated rate constant was obtained by plotting linear regression of ln normalized concentration of Cr(VI) vs time. The resultant rate constant values are depicted in Table 1.

Table 1. Effect of initial Cr(VI) concentration on Cr(VI) reduction rate constants and their half lives for CMC stabilized Fe^o nanoparticles

Initial conc. of Cr(VI) (mg/L)	k_{obs} (min^{-1})	$t_{1/2\ obs}$ (min)	r^2
10	$118.0 \pm 4.0 \times 10^{-3}$	5.88 ± 0.25	0.999
15	$51.0 \pm 4.8 \times 10^{-3}$	13.72 ± 1.33	0.990
20	$40.6 \pm 3.8 \times 10^{-3}$	17.21 ± 1.81	0.997
25	$52.7 \pm 3.2 \times 10^{-3}$	13.22 ± 0.88	0.997

Experimental Conditions: Conc. of Fe^o = 0.2 g/L, Temp = 28 °C, pH = 7, ω = 500 rpm

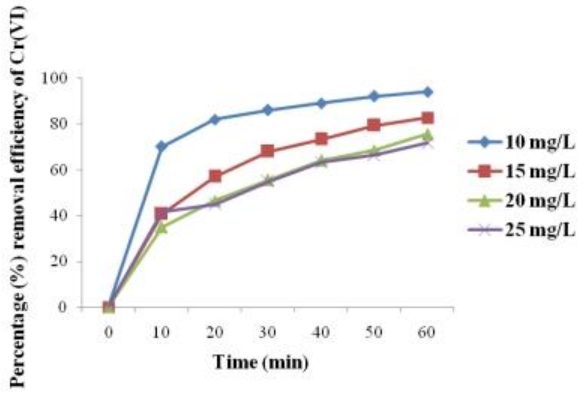

Fig.5. Effect of initial Cr(VI) concentration on Cr(VI) removal efficiency by CMC stabilized Fe^o nanoparticles

It is revealed that rate constant of Cr(VI) removal is decreased with the increase of the initial Cr(VI) concentration. It can be postulated that since Cr(VI) is a strong oxidant and a well-known passivator of Fe^o, as more Cr(VI) came close to the vicinity of Fe^o, more Fe^o would be oxidized and lost their activity leading the decrease in the k_{obs} (Geng *et al.,* 2009).

Effect of Fe^o concentration

The influence of Fe^o concentration on the reduction of Cr(VI) is presented in Fig.6. Four Fe^o nanoparticle concentrations were employed in this study. Fe^o dosage was increased from 0.1g/L to 0.4 g/L, the percentage removal of Cr(VI) increased from 42.0% to 96.0%. This phenomenon is attributed to the increase in the active sites on the CMC-Fe^o surface. It can be concluded that the rate of Cr(VI) binding with adsorbent was greater in the initial stages, then gradually decreased and remained almost constant after an optimum period. It is believed that the Cr(VI) reductive reaction occurs on the Fe^o nanoparticle surfaces. Increase in adsorbent concentration generally increase the level of adsorption of Cr(VI) ions because of an overall increase in surface area of the adsorbent, which in turn increases the number of binding sites (Wang *et al.,* 2010) resulting in high removal efficacy.

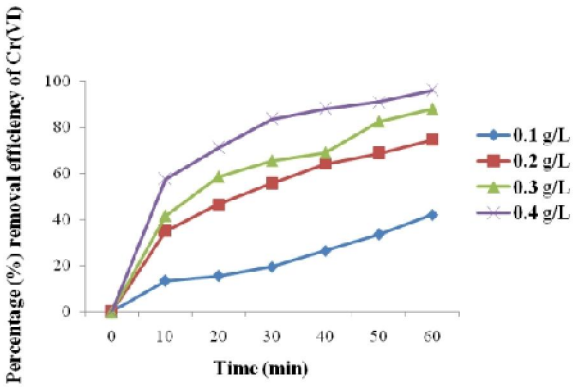

Fig.6. Effect of initial Fe^o concentration on Cr(VI) removal efficiency by CMC stabilized Fe^o nanoparticles

Table 2. Effect of initial Fe^o concentration on Cr(VI) reduction rate constants and their half lives for CMC stabilized Fe^o nanoparticles

Initial conc. of Fe^o(g/L)	k_{obs} (min^{-1})	$t_{1/2\ obs}$ (min)	r^2
0.1	$14.5 \pm 7.6 \times 10^{-3}$	47.94 ± 2.69	0.999
0.2	$51.0 \pm 4.8 \times 10^{-3}$	13.72 ± 1.33	0.999
0.3	$51.2 \pm 4.4 \times 10^{-3}$	13.66 ± 1.34	0.997
0.4	$82.3 \pm 6.9 \times 10^{-3}$	8.48 ± 0.78	0.996

The pseudo first order rate constants are summarized in Table 2. An increase in rate constant (k_{obs}) is noticed from $14.5 \pm 7.6 \times 10^{-3}$ min^{-1} to $82.3 \pm 6.9 \times 10^{-3}$ min^{-1}. It has been noticed that the rate constant increases linearly with the increasing Fe^o concentration but decreases with increasing initial Cr(VI) concentration. It is believed that the Cr(VI) reduction reaction occurs on the Fe^o nanoparticles surfaces.
As the Fe^o nanoparticles mass concentration increases, the reactive Fe sites increased proportionally which lead to the increase of Cr(VI) removal efficiency (Wang *et al.,* 2010).

Effect of pH

The initial pH of the metal solution is an important parameter affecting the adsorption of metal ions. The effect of pH was determined by studying the adsorption of Cr(VI) at initial Cr(VI) concentration of 20 mg/L with adsorbent doses of 0.2 g/L. The effect of initial solution pH on the Cr(VI) removal efficiency using CMC stabilized Fe^o nanoparticles is shown in Fig.7, which shows that maximum adsorption was observed at pH 3 (98.0%). These results showed that Cr(VI) removal was much higher in acidic pH (pH<5) and the acidity of Cr(VI) solution has a major influence on the reduction rate of Fe^o nanoparticles. It is due to the fact that as the media getting acidic, more and more protons will be accumulated on the Fe^o surface and getting more positively charged. The electrostatic attraction between the positive charges of the nanoparticle surface and the negatively charged chromate anion facilitates the adsorption of Cr(VI) and enhances the reduction of Cr(VI) to Cr(III) (Geng *et al.,* 2009). Observed rate constant (k_{obs}) values for the removal reaction at different initial pH values are represented in Table 3. A decrease in k_{obs} is noticed from $64.5 \pm 12.2 \times 10^{-3}$ min^{-1} at pH 3 to $19.0 \pm 1.3 \times 10^{-3}$ min^{-1} at pH 10. This indicated that the rate of Cr(VI) removal process decreases with increasing initial solution pH. The possible reason for that is the formation of iron oxides on the surface of Fe^o passivates the iron surface (Satapanajaru *et al.,* 2008), that hinders the surface reactivity of nanoparticles. Low pH would remove these passivating layers from iron surface and renders it to be free for reaction with the halogenated molecules.

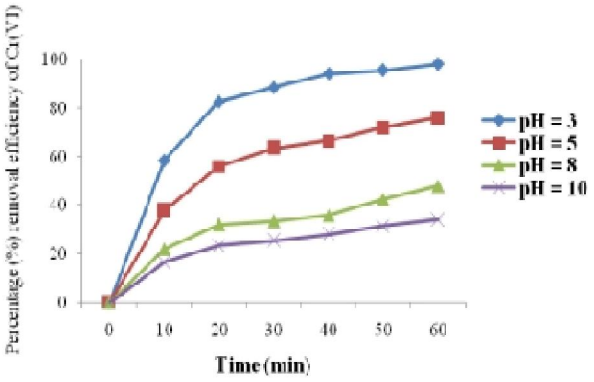

Fig.7. Effect of initial pH on Cr(VI) removal efficiency by CMC stabilized Fe^o nanoparticles

Table 3. Effect of initial pH on Cr(VI) reduction rate constants and their half lives for CMC stabilized Fe^o nanoparticles

Initial pH	k_{obs} (min^{-1})	$t_{1/2\ obs}$ (min)	r^2
3	$64.5 \pm 12.2 \times 10^{-3}$	11.18 ± 2.30	0.996
5	$42.2 \pm 4.8 \times 10^{-3}$	16.65 ± 1.87	0.995
8	$22.3 \pm 2.7 \times 10^{-3}$	31.45 ± 3.48	0.987
10	$19.0 \pm 1.3 \times 10^{-3}$	37.32 ± 2.64	0.997

Experimental Conditions: Conc. of Cr(VI) = 20 mg/L, Conc. of Fe^o = 0.2 g/L, Temp = 28 ^oC, ω = 500 rpm

Effect of temperature

Temperature is an important factor for governing the adsorption process. The percentage of Cr(VI) adsorption was studied as a function of temperature in the range of 15^{o}C to 45^{o}C. An increase in the temperature resulted in increasing Cr(VI) adsorption rate indicating the process to be endothermic. The removal rate increased from 38.5% to 68.0% with increasing the initial temperature of 15^{o}C to 45^{o}C (Fig.8). An increase in temperature is known to increase the diffusion rate of the adsorbate molecules across the external boundary layer and within the pores (Khezmani and Capart, 2005). The enhancement in the adsorption capacity may be due to the chemical interaction between adsorbents and adsorbate, creation of some new adsorption sites or the increased rate of interparticle diffusion of Cr(VI) ions into the pores of the adsorbent at higher temperature (Hameed Mosavian *et al.,* 2009). In this order, calculated rate constant was increased from $12.0 \pm 1.2 \times 10^{-3}$ min^{-1} to $49.0 \pm 4.8 \times 10^{-3}$ min^{-1} with increasing temperature (Table 4). k_{obs} increased as the temperature increases indicating that vibration rate of Cr(VI) increases at higher temperature leading to a higher colloiding frequency between the Cr(VI) with Fe^o surface (Chuang *et al.,* 1995).

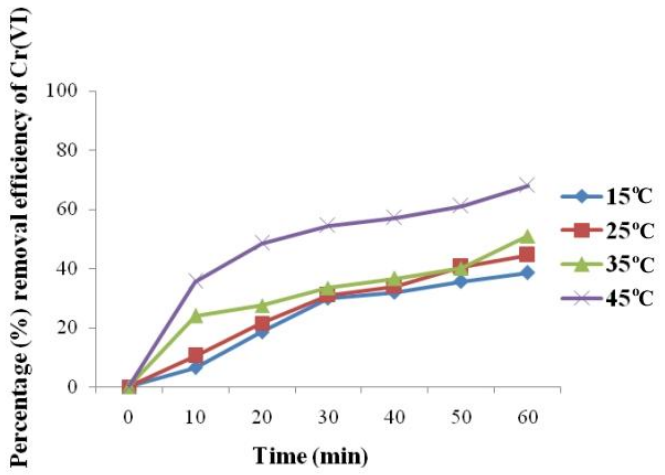

Fig.8. Effect of initial temperature on Cr(VI) removal efficiency by CMC stabilized Fe^o nanoparticles

Effect of different types of Fe^o nanoparticles

Fig.9 shows the removal rate of Cr(VI) by different Fe^o nanoparticles. For starch and CMC stabilized Fe^o nanoparticles the reaction rate was rapid in the first 10 min.

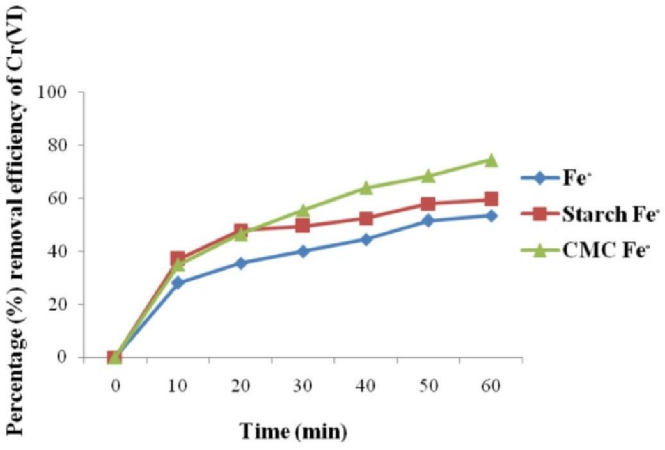

Fig.9. Effect of various types of iron nanoparticles on Cr(VI) removal efficiency

There was an initial sorption phase combined with Cr(VI) reduction, which were enhanced with the increasing surface area of Fe^o nanoparticles. After the first 10 min, the removal rate was significantly slower. The removal efficiency was around 53.5% for Fe^o nanoparticles in 60 min, while 74.5% for CMC stabilized Fe^o nanoparticles. The comparison shows that Fe^o nanoparticles had considerable amount of removal efficiency, but the removal of Cr(VI) from aqueous solution ceased quickly, this may be due to aggregation. The CMC-stabilized Fe^o nanoparticles did not aggregate as much, yielding much increased removal efficiency. He *et al.* (2007) reported that compared to non-stabilized Fe-Pd particles, the CMC stabilized nanoparticles displayed markedly improved stability against aggregation, chemical reactivity and soil transport. It has been proposed that Fe^o nanoparticles reduce Cr(VI) primarily to Cr(III). Then Cr(III) can also precipitate as Fe(II)-Cr(III) hydroxides on the Fe^o nanoparticles surface. The formation of this surface passivation layer on Fe^o nanoparticles accordingly blocked Cr(VI) reduction (Alowitz and Scherer, 2002). For the CMC stabilized Fe^o nanoparticles, CMC can inhibit aggregation of the iron nanoparticles and possibly inhibit the formation of Fe(III)-Cr(III) precipitation (Wang *et al.,* 2010) which results in enhanced removal efficiency.

Table 4. Effect of initial temperature on Cr(VI) reduction rate constants and their half lives for CMC stabilized Fe^o nanoparticles

Initial temp (°C)	k_{obs} (min^{-1})	$t_{1/2\ obs}$ (min)	r^2
15	$12.0 \pm 1.2 \times 10^{-3}$	58.33 ± 6.03	0.997
25	$16.0 \pm 1.4 \times 10^{-3}$	44.13 ± 4.26	0.993
35	$27.0 \pm 1.3 \times 10^{-3}$	25.73 ± 1.23	0.999
45	$49.0 \pm 4.8 \times 10^{-3}$	14.17 ± 1.25	0.986

Experimental Conditions: Conc. of Cr(VI) = 20 mg/L, Conc. of Fe^o = 0.2 g/L, pH = 7, ω = 500 rpm

Table 5. Adsorption isotherm constants for Cr(VI) reduction by CMC stabilized Fe^o nanoparticles

Langmuir constants			Freundlich constants		
Q_m	K_a	R^2	K_f	n	R^2
0.551	0.178	0.999	1.0	1.398	1

Adsorption isotherms

In this study, the Langmuir and Freundlich adsorption models have been successfully applied to investigate the adsorption efficacy of Cr(VI) on the Fe^o surface. Figs. 10-11 demonstrate the linear plot of both isotherm models for Cr(VI) adsorption by CMC stabilized Fe^o nanoparticles. The empirical constant values of the Langmuir and Freundlich isotherms for Cr(VI) adsorption were calculated from the linear plot (Table 5). The data indicates that both the isotherm models presented good fits for all studied parameters ($R^2 > 0.98$). Results indicated that both the isotherms were adequate for describing the Cr(VI) removal because there was no considerable difference between them. This was confirmed by the R^2 value of each model.

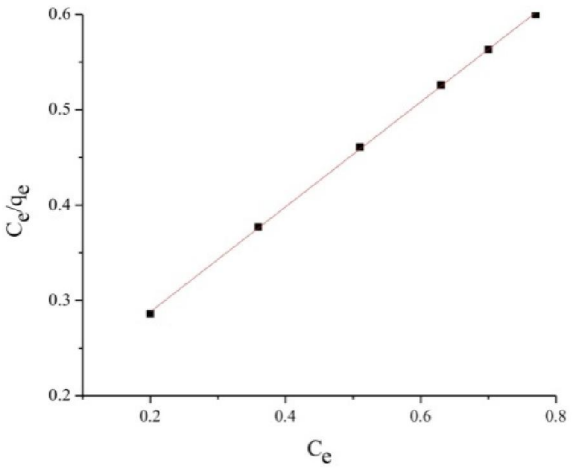

Fig.10. Langmuir isotherm plot for Cr(VI) adsorption by CMC stabilized Fe^o nanoparticles

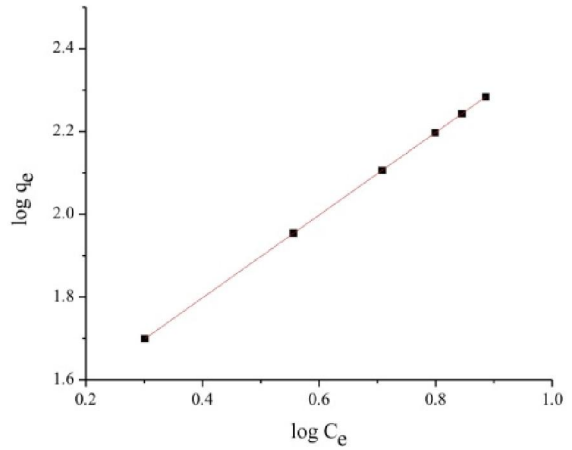

Fig.11. Freundlich isotherm plot for Cr(VI) adsorption by CMC stabilized Fe^o nanoparticles

Conclusion

The reduction of Cr(VI) by Fe^o nanoparticles has received increasing attention in recent years. This study investigate the feasibility of using Fe^o nanoparticles to reduce Cr(VI) in aqueous solution using potassium dichromate as the model contaminant. The data obtained from this work supports the view that the CMC stabilized Fe^o nanoparticles is an effective and low cost adsorbent for the removal of Cr^{6+} from aqueous solution. The adsorption of metal ions is dependent on Cr(VI) concentration, Fe^o concentration, pH and temperature. The CMC stabilized Fe^o nanoparticles exhibited higher removal efficiency than those prepared without a stabilizer because CMC acted as a good dispersant to prevent Fe^o nanoparticles from agglomeration. The pseudo first order kinetic model accurately described adsorption kinetics. Best fitting of equilibrium data with both Langmuir and Freundlich isotherms indicates the applicability of monolayer coverage of Cr on Fe^o surface. Thus the results from our study suggested that Fe^o nanoparticles, especially those stabilized by CMC, could lead to high removal efficacy for applications such as *in situ* remediation of Cr(VI) contaminated soil and water.

Acknowledgements

The authors are very grateful for the financial support provided by Ministry of Science & Technology, DST, Govt. of India for INSPIRE program (Dy.No.100/IFD/10706/) under Assured Opportunity for Research Carrier (AORC), VHNSN College Managing Board, Virudhunagar for providing facilities, Central instrumentation facility, Pondicherry University, Pondicherry and Alagappa University, CECRI, Karaikudi for their technical assistance.

REFERENCES

Aksu, Z. 2002. Determination of the equilibrium, kinetic and thermodynamic parameters of the batch biosorption of nickel (II) ions onto *Chlorella vulgaris*. *Process Biochem*.,38(1):89-99.

Alowitz, M.J. and Scherer, M.M. 2002. Kinetics of nitrate, nitrite, and Cr(VI) reduction by iron metal. *Environ. Sci. Technol*., 36(3): 299-306.

Basha, S., Murthy, Z.V.P. and Jha, B. 2008. Biosorption of hexavalent chromium by chemically modified seaweed, *Cystoseira indica. Chem. Eng. J*., 137(3): 480-488.

Chuang, F.W., Larson, R.A. and Wessman, M.S. 1995. Zero-valent iron-promoted dechlorination of polychlorinated biphenyls. *Environ. Sci. Technol*., 29(9): 2460-2463.

Franco, D.V., Da Silva, L.M. and Jardim, W.F. 2009. Reduction of hexavalent chromium in soil and ground water using zerovalent iron under batch and semi-batch conditions. *Water Air Soil Poll*., 197(1-4): 49-60.

Geng, B., Jin, Z.H., Li, T.L. and Qi, X.H. 2009. Preparation of chitosan-stabilized Fe^o nanoparticles for removal of hexavalent chromium in water. *Sci. Total Environ*., 407(18): 4994-5000.

Hameed Mosavian, M.T., Khazaei, I. and Aliabadi, M. 2009. Removal of chromium (VI) from aqueous solution by adsorption using *Cousinia eryngioides* bios and activated carbon. *Iran. J. Earth Sci.*, 1(1): 35-43.

He, F. and Zhao, D. 2005. Preparation and characterization of new class of starch-stabilized bimetallic nanoparticles for degradation of chlorinated hydrocarbons in water. *Environ. Sci. Technol*., 39(9): 3314-3320.

He, F., Zhao, D., Liu, J. and Roberts, C.B. 2007. Stabilization of Fe-Pd nanoparticles with sodium carboxymethyl cellulose for enhanced transport and dechlorination of trichloroethylene in soil and ground water. *Ind. Eng. Chem. Res*., 46(1): 29-34.

Hu, X.J., Wang, J.S., Liu, Y.G., Li, X., Zeng, G.M., Bao, Z.L., Zeng, X.X., Chen, A.W. and Long, F. 2011. Adsorption of chromium (VI) by ethylenediamine-modified cross-linked magnetic chitosan resin: Isotherms, kinetics and thermodynamics. *J. Hazard. Mater*., 185(1): 306-314.

Karthikeyan, T., Rajgopal, S. and Miranda,L.R. 2005. Chromium (VI) adsorption from aqueous solution by *Hevea brasilinesis* sawdust activated carbon. *J. Hazard. Mater B*., 124(1-3):192-199.

Khezami, L. and Capart, R. 2005. Removal of chromium (VI) from aqueous solution by activated carbons: Kinetic and equilibrium studies. *J. Hazard. Mater*., 123(1-3): 223-231.

Lazaridis, N.K. and Asouhidou, D.D. 2003. Kinetics of sorptive removal of chromium (VI) from aqueous solutions by calcined Mg-Al-CO_3 hydrotalcite. *Water Res*., 37(12): 2875-2882.

Li, Y.H., Di, Z., Ding, J., Wu, D., Luan, Z. and Zhu, Y. 2005. Adsorption thermodynamic, kinetic and desorption studies Pb^{2+} on carbon nanotubes. *Water Res*., 39(4): 605-609.

Lin, C.L., Lee, C.F. and Chiu, W.Y. 2005. Preparation and properties of poly (acrylic acid) oligomer stabilized superparamagnetic ferrofluid. J. Colloid. Interf. Sci., 291(2): 411-420.

Magdassi, S., Bassa, A., Vinetsky, Y. and Kamyshny, A. 2003. Silver nanoparticles as pigments for water-based ink-jet inks. *Chem. Mater*., 15(11): 2208-2217.

Malkoc, E. 2006. Ni(II) removal from aqueous solutions using cone biomass of *Thuja orientalis. J. Hazard. Mater*., 137(2): 899-908.

Ponder, S.M., Darab, J.G., Bucher, J., Caulder, D., Craig, I., Davis, L., Edelstein, N., Lukens, W., Nitsche, H., Rao, L., Shuh, D.K. and Mallouk, T.E. 2001. Surface chemistry and electrochemistry of aqueous metal contaminants. *Chem. Mater*., 13(2): 479-486.

Satapanajaru, T., Anurakpongsatorn, P., Pengthamkeerati, P. and Boparai, H. 2008. Remediation of atrazine contaminated soil and water by nanozerovalent iron. *Water Air Soil Poll*., 192(1-4): 349-359.

Schrick, B., Blough, J.L., Jones, A.D. and Mallouk, T.E. 2002. Hydrodechlorination of trichloroethylene to hydrocarbons using bimetallic nickel-iron nanoparticles. *Chem. Mater*., 14(12): 5140-5147.

Shen, Y.S., Wang, S.L., Tzou, Y.M., Yan, Y.Y. and Kuan, W.H. 2012. Removal of hexavalent Cr by coconut coir and derived chars- The effect of surface functionality. *Bioresour. Technol*., 104: 165-172.

Si, S., Kotal, A., Mandal, T., Giri, S., Nakamura, H. and Kohara, T. 2004. Size-controlled synthesis of magnetite nanoparticles in the presence of polyelectrolytes. *Chem. Mater*., 16(18): 3489-3496.

Simmin, R.G., Schoch, A.B. and Barun, P.V. 2004. Polymer size and concentration effects on the size of gold nanoparticles capped by polymeric thiols. Langmuir, 20(13): 5613-5620.

Singh, R., Misra, V. and Singh, R.P. 2011. Synthesis, characterization and role of zero-valent iron nanoparticle in removal of hexavalent chromium from chromium-spiked soil. *J. Nanopart*. Res., 13(9): 4063-4073.

Tiraferri, A. and Sethi, R. 2008. Enhanced transport of zerovalent iron nanoparticles in saturated porous media by guar gum. *J. Nanopart. Res*., 11(3): 635-645.

Wang, C.B. and Zhang, W.X. 1997. Synthesizing nanoscale iron particles for rapid and complete dechlorination of TCE and PCBs. *Environ. Sci. Technol*., 31(7): 2154-2156.

Wang, Z., Peng, P. and Huang, W. 2009. Dechlorination of γ-hexachlorocyclohexane by zero-valent metallic iron. *J. Hazard. Mater*., 166(2-3): 992-997.

Wang, Q., Huijing, Q., Yueping, Y., Zhen, Z., Cissoko, N. and Xinhua, X. 2010. Removal of hexavalent chromium by carboxymethyl cellulose stabilized zero-valent iron nanoparticles. *J. Contam. Hydrol*., 114(1-4): 35-42.

Wielinga, B., Mizuba, M. and Hansel, C.M. 2001. Iron promoted reduction of chromate by dissimilatory iron-reducing bacteria. *Environ. Sci. Technol*., 35(3): 522-527.

Yuvakumar, R., Elango, V., Rajendran, V. and Kannan, N. 2011. Preparation and characterization of zerovalent iron nanoparticles. Dig. *J. Nanomater. Bios*., 6(4): 1771-1776.

Zhu, B.E., Lim, T.T. and Feng, J. 2006. Reductive dechlorination of 1,2,4- trichlorobenzene with palladized nanoscale Fe^o particles supported on chitosan and silica. Chemosphere, 65(7): 1137-1146.

****